LINER PAPER WITH HIGH AIR PERMEABILITY, HIGH WET STRENGTH, ANTI-MILDEW AND ANTIBACTERIAL PROPERTIES FOR LIQUID CRYSTAL GLASS

SIJIE ZHUANG,[*,**,***] WENZHI LV,[****] JINGXIAN ZHANG,[*,**,***] ZHU LONG,[*,**,***] CHANG SUN,[*,***] XUEFENG LU[*,***] and SHUANGFEI WANG[**]

[*]*Key Laboratory of Eco-Textiles, Ministry of Education, Jiangnan University, Jiangsu Wuxi 214122, China*
[**]*Guangxi Key Laboratory of Clean Pulp and Papermaking and Pollution Control, Nanning 530004, China*
[***]*Papermaking Laboratory, Jiangnan University, Jiangsu Wuxi 214122, China*
[****]*College of Chemistry and Chemical Engineering of Qiannan Normal University for Nationalities, Tuyun 558000, China*
✉ *Corresponding authors: Z. Long, longzhu@jiangnan.edu.cn*
S. Wang, wangsf@gxu.edu.cn

Received June 27, 2022

In this paper, we report a method for the preparation of liner paper applied on liquid crystal glass. It was obtained by wet forming of hardwood fiber and a laboratory-made hydrophilic dispersible polyester staple fiber in a certain proportion. The laboratory-made hydrophilic dispersible polyester staple fiber was obtained by co-deposition of gallic acid and ethylenediamine on PET fiber. Some additives were used in the papermaking process, including wet strength agent polyamide epichlorohydrin (PAE), anti-mildew and antibacterial agent polyhexamethylene biguanide (PHMB), and pH adjuster boric acid (H_3BO_3). Results showed that the liner paper has high air permeability (~35.99 μm.(Pa·s)$^{-1}$), good wet strength (~0.720 kN.m^{-1}) and excellent anti-mildew and antibacterial properties. Interestingly, the pore size of the modified PET fiber paper increased between 23% and 29% within the same pore size range compared with PET fiber paper. This provides a theoretical basis for the relationship between paper pore size and air permeability.

Keywords: wood fiber, polyester staple fiber, paper air permeability, hydrophilic dispersibility, liquid crystal glass liner paper

INTRODUCTION

Liquid crystal glass liner paper requires a smooth and delicate surface, free of scratches and without dust, impurities, lint, or powder, when used as separation paper between LCD screens. It is used as a lining to decrease friction between the glass layers. It also needs to have anti-mold and moisture-proof properties,[1] so that it can inhibit the growth of mold when used as a glass interlayer for corrosion resistance and to effectively protect the film surface of the glass. The existing raw materials for making liquid crystal glass spacer papers are mostly pure wood pulps, for which it is difficult to ensure that the wet strength is retained with a certain degree of air permeability. This problem can be solved by introducing an appropriate amount of chemical fibers.

Polyethylene terephthalate (PET) fiber is widely used in pulp and paper, textiles, food packaging, construction and other fields, as it is chemically stable, rigid, has high breaking strength and has temperature resistance.[2,3] However, the surface of the PET fiber is straight and smooth, with few wrinkles parallel to the axial direction. The low specific surface area can lead to insufficient hydrophilicity and dispersibility of the PET fiber, which limits its combination with cellulose fibers. Therefore,

improving the wetting and dispersibility of PET fibers by their modification is of great significance to wet-laid papermaking.

Surface chemical or physical modifications have become the main technological methods for modifying PET fibers. Wu *et al.* used cutinase to modify PET fiber and confirmed that the hydrolysis of the ester bond produced a large number of carboxyl and hydroxyl groups on the fiber surface.[4] These greatly improved the wettability and hydrophilicity of the PET fiber fabric, along with its mechanical strength, so that there was no damage to performance. Abdelghaffar *et al.* used three different plasma gases to treat the PET fabric, followed by the quaternary ammonium salt cation treatment. The average roughness of the PET fabric surface improved, the etching was more obvious, and the hydrophilicity increased.[5] Therefore, it is possible to improve the hydrophilic wettability of the fiber without damaging the inherent properties through a green and simple modification that is compatible with the fiber.

Gallic acid, *i.e.*, 3,4,5-trihydroxybenzoic acid, is a natural polyphenol compound widely used in biology, medicine, chemical industry and other fields.[6–9] It is a natural degradable alternative to environmentally unfriendly raw materials. Its preparation is simple and fast, and the solution used is non-toxic or has low toxicity. Its polyphenol structure has the ability to be modified similarly to dopamine and it is low cost. Therefore, it is considered as a potential dopamine substitute. Ethylenediamine is a primary amine and building block that can be used as a chain extension module.

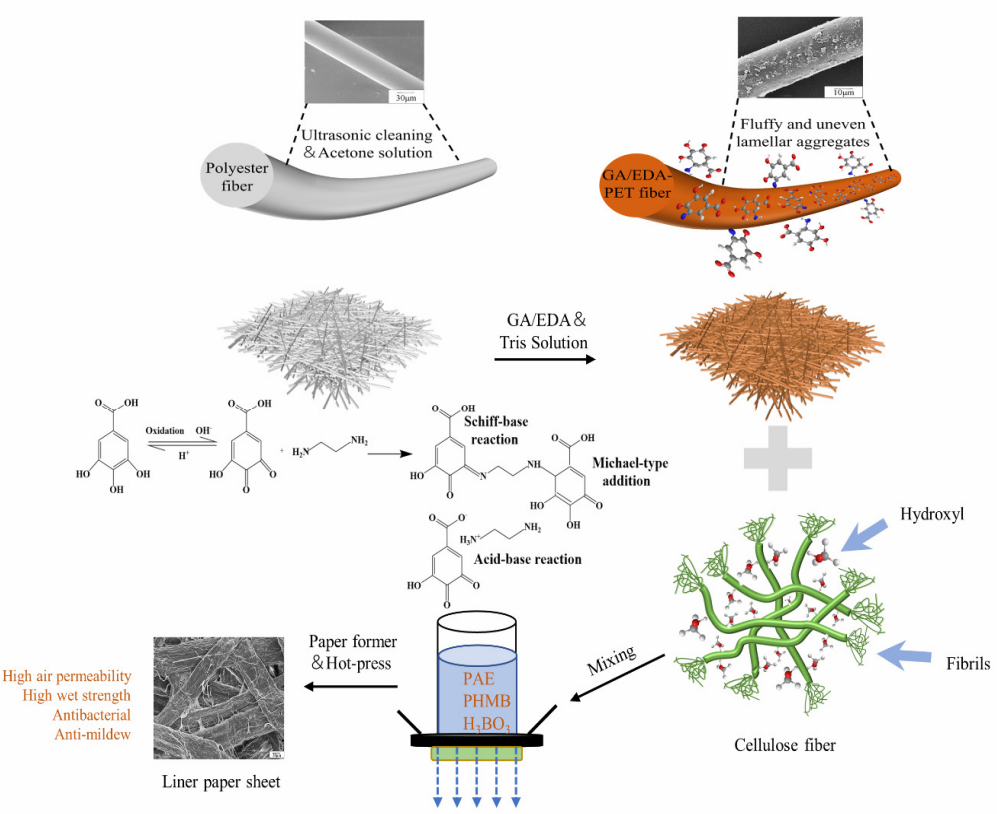

Figure 1: Schematic diagram of potential co-deposition modification mechanism of PET chopped fiber and paper-forming process

As shown in Figure 1, gallic acid will be oxidized into quinone compounds under alkaline conditions due to its pyrogallol structure. A potential Michael addition reaction or Schiff base reaction will occur by adding a certain amount of ethylenediamine to make them both co-deposit on the surface of the PET fiber. This is expected to increase the surface polarity of the PET fiber, increase the surface roughness, and improve the wetting performance of the fiber.

EXPERIMENTAL

Main materials

Polyethylene terephthalate (PET) chopped fibers (3.0 mm length, 2.0 D fineness, 240.0-260.0 □ melting point, 5.5 GPa breaking strength, 20%-30% elongation at break) were obtained from Jinkeli Special Fiber Co. Ltd. (Zibo, China). P-toluenesulfonic acid (PTS; ≥98%) was purchased from Aibi Chemical Reagent Co. Ltd. (Shanghai, China). Bleached hardwood and softwood kraft pulp boards were purchased from Kunshan Banknote Paper Co. Ltd. (Kunshan, China). Gallic acid monohydrate (GA), ethylenediamine (EDA) (content 99%), trimethylolaminomethane (Tris) (biochemical reagents), acetone, absolute ethanol, hydrochloric acid, boric acid, lithium chloride, calcium chloride, potassium carbonate, sodium bromide, sodium chloride and zinc sulfate were all analytically pure, provided by Sinopharm Chemical Reagent Co. Ltd. (Shanghai, China), and used without further purification. Polyhexamethylene biguanide (PHMB) was provided by Keweihong Environmental Technology Co. Ltd. (Tianjin, China). Wet strength agent (polyamide epichlorohydrin resin, PAE) was commercially available. All solutions were made using deionized water.

Pretreatment of short-chopped polyester fibers

The PET fibers were cleaned ultrasonically three times in a 1:20 acetone to bath ratio solution for 30 minutes each time to remove the spinning oils and other impurities from their surfaces. The PET fibers were washed several times in deionized water and dried in a vacuum oven at 65 °C for 12 h.

Orthogonal experimental design

To improve the experimental efficiency, a preliminary investigation focused on factors affecting the surface-coating of PET fibers to determine the GA mass concentration (A), reaction time (B), and GA/EDA ratio (C), without considering the interactions among these factors. An orthogonal design involving the three factors and three levels was prepared for the experiment and the contact angle (CA) of the PET fibers in deionized water was used as the evaluation standard. These results were analyzed using the range analysis method.

The reaction parameters were optimized experimentally as given in Table 1, and the surface-coating experiment was performed using this optimized combination scheme.

Preparation of gallic acid/EDA co-deposition on cross-linked modified short-chopped polyester fibers

Tris-hydroxymethylaminomethane (0.6057 g) was added to 50 mL of deionized water for the 0.1 M Tris solution. An appropriate amount of hydrochloric acid was added to adjust the pH to 8.5, yielding a Tris-HCl buffer solution. A certain mass ratio of GA and EDA was fully dissolved in deionized water and the Tris-HCl buffer was added to obtain a GA/EDA reaction solution. The pretreated PET fibers were pre-wetted with absolute ethanol and immersed in the reaction solution. The reaction was then magnetically stirred at 25 °C for a certain period of time. Finally, the modified PET fibers were washed with ethanol and deionized water and dried in a vacuum oven at 65 °C for 12 h. The thus-obtained modified PET fibers will be further denoted as GA/EDA-PET.

Preparation of liquid crystal glass spacer paper

The bleached kraft pulps (hardwood pulp and softwood pulp) were disintegrated with a Valley beater (PL4-3, Xianyang Test Laboratory Equipment Co. Ltd., China) and the moisture content was balanced to prepare a slurry with pulp consistency of 10%, which was ground to 24 °SR (hardwood pulp) and 32 °SR (softwood pulp) in a vertical PFI refiner (PL11, Xianyang Test Laboratory Equipment Co. Ltd., China). The two pulps were put in a sheet paper machine (IMT-SJ01, Dongguan International Materials Testing Equipment Co. Ltd., China), according to a certain ratio, for 5 minutes. The laboratory-made GA/EDA-PET, pH regulator (H_3BO_3), antibacterial agent (PHMB), wet-strength agent (PAE), and other related papermaking auxiliaries were added to the sheet paper machine. The final liner paper was obtained by dehydration forming, pressing with 0.4 Mpa, and drying at 105 °C. The paper basis weight was set to 60 g/m^2.

Table 1
Orthogonal experimental factors and levels

Levels	Factors		
	GA mass concentration, g/L	Time, h	GA/EDA ratio
1	0.8	6	1:1
2	1.0	12	2:1
3	1.2	24	4:1

The hardwood pulp beaten at 24 °SR and softwood pulp at 32 °SR were made into paper, according to an 8:2 ratio, which was recorded as paper A. The hardwood pulp (24 °SR) and laboratory-made

hydrophilic polyester short fiber in a ratio of 8:2, with 21 μs/cm water conductivity, 1.5% boric acid dosage, and 0.6% wet strength agent dosage (PAE), were made into paper recorded as paper B. These percentages were both relative to absolute dry pulp weight. An antibacterial agent (PHMB) was added during the forming process of paper B to make paper C, with 0.3% mass relative to the bone-dry pulp.

Characterization

Fourier transform infrared spectroscopy (FTIR). The chemical structures of the PET fibers before and after the treatment were characterized via FTIR (Nicolet iS10, Thermo Fisher Scientific Co., Ltd.). Sixteen scans in the 500–4000 cm^{-1} range with a resolution of 4 cm^{-1} were recorded.

X-ray photoelectron spectroscopy (XPS). An X-ray photoelectron spectrometer (Thermo Scientific K-Alpha, Thermo Fisher Scientific Co., Ltd.) was used to measure the surface element composition and functional group changes of the fiber before and after the treatment. The curve of the N 1s peak pattern was fit using the least square method.

Scanning electron microscopy (SEM). A SEM (SU151, Hitachi Ltd., Japan) was used to observe the microscopic appearance of the fiber surfaces before and after the treatment and to conduct a comparative analysis. A silver-containing conductive adhesive sheet was used as the base surface and was tested after gold spray treatment. The voltage value was 20 kV.

Wettability test. The carded PET fibers before and after the fiber treatment were placed in a parallel arrangement on a 1.5×1.5 cm polytetrafluoroethylene board. The fibers were then spread and flattened with an oil press to make the fiber bundle sample, which was placed in the tensiometer (DCAT-21, German Dataphysics Ltd.) The deionized water droplet size was 2 μL. The video method was used to test the contact angle between the small molecule liquid and the fiber assembly. The contact angle was recorded first at 1 s and then every 2-4 s after the droplet formation. The average value was taken as the test liquid static contact angle on the sample.

Fiber distribution in polyester fiber. A 3×3 cm sample was cut from the PET fiber paper and the pore size distribution of the fiber paper was measured using a porous material pore size analyzer (CFP-1100A, PMI Co., Ltd.).

Paper antibacterial test. E. coli O157: H7 (ATCC 43895) and *Staphylococcus aureus* (ATCC 6538) were used as test strains to conduct antibacterial tests on paper sheets according to the revised AATCC 100-2004 standards.

Paper mildew resistance test. Different saturated salt solutions were prepared for producing different relative humidities for the liner paper sandwiched between the glass sheets at 65 °C. The moldiness of the glass was observed according to the "visual appearance method" introduced by H.V. Walters and P.B. Adams in the United States to judge the degree of moldiness.[10]

Paper performance test. According to GB/T 12914-2008, GB/T 454-2002 and GB/T 458-2008, the tensile index, burst index, and paper air permeability were measured, respectively.

To test the wet paper web strength, the sample was immersed in water at a temperature of 23 ± 1 □. The center was soaked and both ends were kept dry. The sample was bent into a ring with the center part down and again immersed in water until the water evenly touched the full width of the paper strip and soaked the upper surface. The wetted length included between 25 and 50 mm of the central part. The sample was immersed in water for 1 minute, taken out, gently patted dry, and placed on the tensile strength tester.

RESULTS AND DISCUSSION

Process optimization of GA/EDA co-deposition on short-chopped PET fibers

The results of the L_9 (3^3) orthogonal experiment conducted on the GA/EDA co-deposition on short-chopped PET fibers, as well as the CA results, are listed in Table 2. It can be seen from the "*R*" value that the largest influence on the contact angle is the GA/EDA mass ratio, followed by GA mass concentration, and then reaction time. Excessive EDA inhibits the formation of covalent bonds between aromatic rings and reduces the π-π stacking effect between pyrogallol polymer molecules,[11] which eventually stops the deposition of particles. The best conditions observed from the contact angle measurements are a GA mass concentration 1.0 g/L, a GA/EDA mass ratio of 2:1, a reaction time of 6 h, and a reduction of the contact angle of PET fiber to deionized water by 57.2°. A follow-up performance test was done using PET-4.

Fiber surface elements and changes in functional groups

Figure 2 shows the infrared spectrum of PET fiber before and after the co-deposition of gallic acid and ethylenediamine. The PET fiber before and after the modification has strong absorption peaks at 1711, 1242, 1091 and 722 cm^{-1}, which correspond to C=O stretching, C-O-C asymmetric and symmetric stretching, and -CH_2-methylene bending vibrations, respectively.[12]

The infrared spectrum of the PET fiber changes after co-deposition and new characteristic absorption peaks appear at 1654 and 1566 cm^{-1} (Fig. 2b), which correspond to the C=N stretching and N-H bending vibrations, respectively. The C=N stretching peaks are produced by the

reaction of GA and EDA. The pyrogallol group in GA can interact with various substrates to form an "anchor point". Meanwhile, it can form a covalent bond through an oxidative coupling reaction. Intermolecular interactions can also form non-ferrous bonds through hydrogen bonding and π-π stacking in the covalent cross-linked structure.[13]

Table 2
Orthogonal experiment results L_9 (3^3)

Sample	GA mass concentration, g/L	Time, h	GA/EDA mass ratio	Contact angle, °
PET-0	-	-	-	119.3
PET-1	0.8	6	1:1	75.8
PET-2	0.8	12	2:1	63.6
PET-3	0.8	24	4:1	68.4
PET-4	1.0	6	2:1	62.1
PET-5	1.0	12	4:1	71.4
PET-6	1.0	24	1:1	75.9
PET-7	1.2	6	4:1	65.3
PET-8	1.2	12	1:1	78.7
PET-9	1.2	24	2:1	85.2
I	207.8	203.2	230.4	Contact angle can be reduced by up to 57.2°
II	209.4	213.7	210.9	
III	229.2	205.1	205.1	
R	21.2	10.5	25.3	

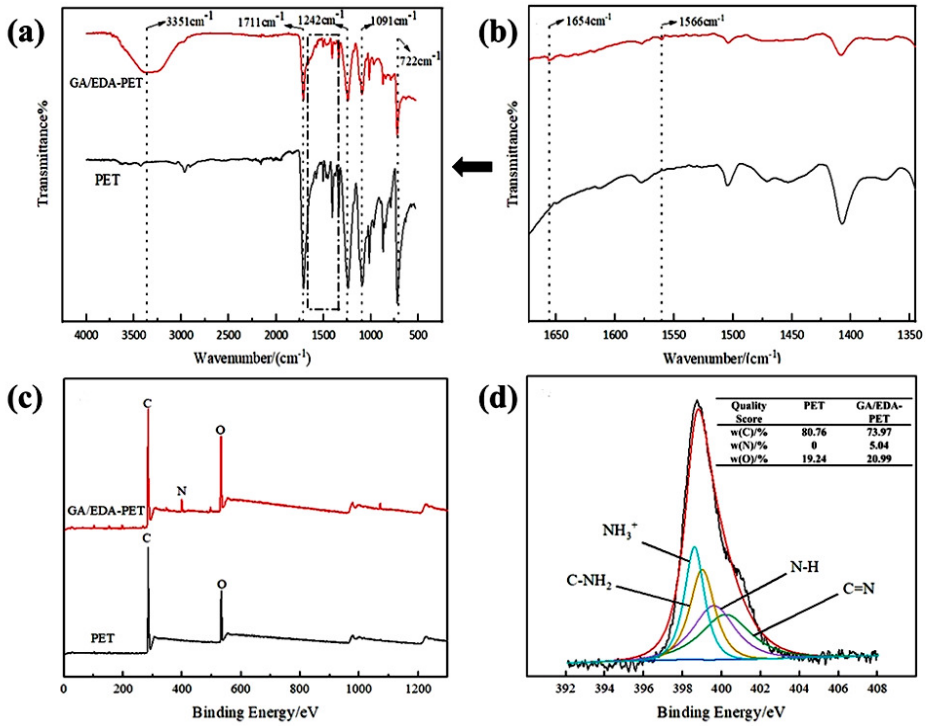

Figure 2: (a) Full infrared spectra, (b) partial infrared spectra and (c) wide-scan X-ray photoelectron spectroscopy (XPS) spectra of fibers before and after PET co-deposition modification; (d) N 1s peaks in the analytical spectra of GA/EDA-PET fibers

The carbonyl group in the quinoid structure can undergo a nucleophilic addition reaction after oxidation with the primary amine in EDA. The lone electron pair in the primary amine attacks the positively charged carbon atom in the carbonyl group and forms an intermediate α-hydroxyamine

compound, which can be further dehydrated to form a C=N bond, indicating that a potential Schiff base reaction has occurred.[14] Alternatively, the carbonyl group is a strong electron withdrawing group that can cause the electron density of the carbon atoms in the methylene group to decrease. EDA is prone to losing protons in the alkaline Tris buffer solution to form a relatively stable carbanion, which acts as a nucleophilic and co-electrophilic group, such as a quinone group and a benzene ring. The addition reaction of the conjugate system forms an N-H bond. Meanwhile, a wide absorption peak appearing at 3351 cm^{-1} is identified as the stretching vibration of the hydroxyl group (-OH) on the GA molecular chain. This also explains the growth of the carbon chain and is the biggest feature that proves the potential Michael addition reaction has occurred. The above results proved that GA/EDA is co-deposited on the surface of PET fibers.

Figure 2c shows the XPS full scan view of the fiber before and after the co-deposition. The PET fiber before the treatment has C 1s and O 1s peaks, but no N 1s peak. However, the treated PET fiber has the N 1s peak, while the O 1s peak is more pronounced, the former increased significantly and the intensity of the C 1s peak decreased, which is consistent with the results from the infrared spectra.

Figure 2d shows the N 1s peak fitting map obtained by the XPS Peak Fit software. Nitrogen appears and reaches 5.04% abundance after the treatment due to the potential Michael addition or Schiff base reaction of gallic acid and ethylenediamine, which is co-deposited and grafted on the surface of the fiber to add a large amount of nitrogen. The O 1s content increased from 19.24% to 20.99%, which also indicated the occurrence of co-deposition grafting. The treated fiber showed NH_3^+ and C-NH_2 from the acid-base neutralization reaction with the peaks at 398.6 and 399 eV, which might not react, but were connected with the benzene ring. The new peak at 398.8 eV corresponded to the amide obtained from the potential Michael addition reaction. The -NH- structure in the amine compound, 400.5 eV corresponds to the -C=N- structure in the benzene ring compound. This is because of the potential Schiff base reaction, which further proves that GA/EDA is co-deposited on the surface of the PET fiber.

Changes in fiber and paper surface microtopography

The surface microtopographies of PET and GA/EDA-PET fibers are shown in Figure 3. The surface of the PET fiber after ultrasonic cleaning with acetone was smooth and flat, without etching, protrusions or grooves, and the fiber is cylindrical (Fig. 3a). The modified PET fibers are shown in Figure 3b-d with rough and convex surfaces. The aromatic ring of GA can form a π-π interaction with other benzene rings, which can enhance the adhesion to the surface of aromatic rich compounds.[15,16] Protonated amines can also establish cation-π interactions that can enhance the adsorption of GA on charged surfaces and the cohesion of materials rich in aromatic and cationic functional groups.[17,18] This can generate a large number of fluffy, curved, and uneven layered aggregates that adhere tightly to the smooth PET fiber to make the surface of the PET fiber rougher. Meanwhile, the polarity of the fiber surface increases because the coating contains abundant hydroxyl groups and the hydrophilic properties of the fiber are improved further. It can be seen from Figure 3e and e' that the PET fibers have a smooth surface and are only interspersed and arranged in the middle of the rough-surfaced hardwood fibers. This is because the PET fibers have a smooth surface, poor hydrophilicity and dispersibility, and cannot form with hardwood fibers. Strong intermolecular forces, such as hydrogen bonds, lead to different pore sizes in paper. It can be seen from Figure 3f and f' that the coarser GA/EDA-PET fibers have a rough surface, and certain fiber bonding points with hardwood fibers, while the bonding effect and paper evenness are better.

Stability of fiber in acid-base environment and paper pore size distribution

Generally, the co-deposition coating is easily damaged under harsh and unfavorable conditions, such as acid-base environment, organic solvent, high temperature and high humidity, and corrosive solution. Figure 4a shows that the coating is largely peeled off with time in an alkaline environment, which may be due to the destruction of the π-π interaction between the aromatic ring of gallic acid and the benzene ring of PET, which reduces the adhesion to the surface of aromatic compounds. Although the contact angle is improved in an acidic environment, it still maintains a good hydrophilic effect. It is

conducive to the suitability of an acidic papermaking environment for liner paper.

The fiber dispersion effect determines the uniformity of the paper pore diameter. Figure 4b shows the pore size distribution of 24 °SR hardwood pulp and PET fibers before and after modification at a ratio of 9:1. The fiber dispersibility in the paper sheet prepared by mixing untreated PET fiber and hardwood pulp is poor, and 6.5% to 8.5% is distributed in every 40 μm between 200 and 760 μm (Fig. 4b).

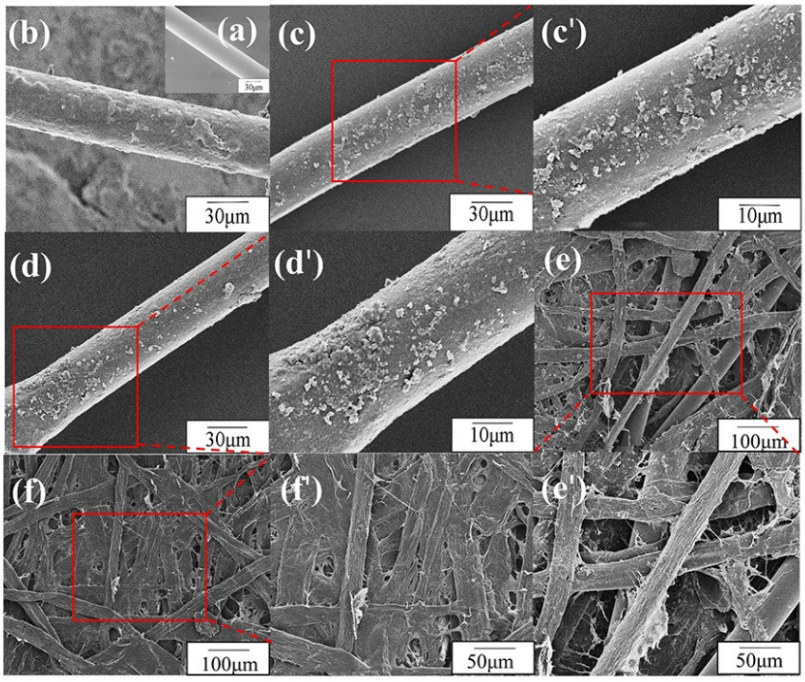

Figure 3: Scanning electron microscopy (SEM) images of PET fiber (a), GA/EDA-PET fiber (b), (c), (c'), (d), (d'); paper sheet from mixed PET fiber and plant fiber (e), (e'); paper sheet from mixed GA/EDA-PET fiber and plant fiber (f), (f')

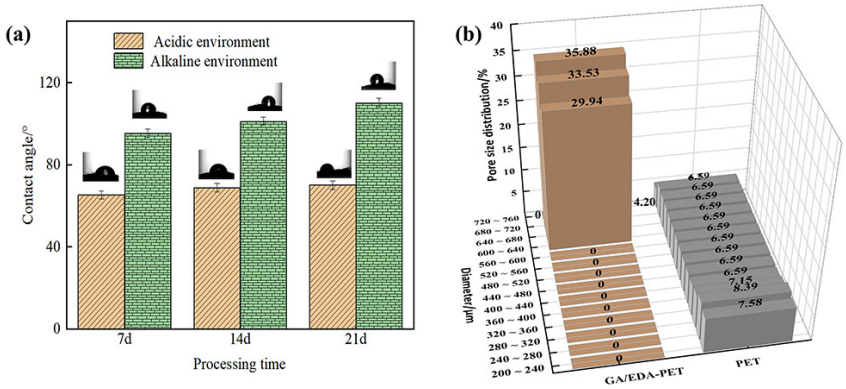

Figure 4: (a) Changes of contact angle of GA/EDA-PET fibers in acid-base environment at 7, 14 and 21 days; (b) Pore size distribution of fibers in paper

The size of the pores formed among the fibers was different and the uniformity of the paper was poor. The PET fiber will be entangled when it is dispersed and gathered into a “cluster” with only a few single fibers distributed. This results in uneven hydrogen bonding during paper formation and affects the uniformity and mechanical properties of the paper.

In contrast, the pore size of the GA/EDA-PET fiber paper is distributed between 600 and 720 μm. Pores with diameters between 600 and 640 μm account for 29.94%, diameters between 640

and 680 μm account for 33.53%, and diameters between 680 and 720 μm account for 35.88%. The pore size increased between 23% and 29% in the same range as PET fiber was turned into paper, which indirectly indicates that the fiber dispersion effect after modification is better because the modified fiber has a large number of hydroxyl groups on the surface that increase the hydrophilicity and are evenly dispersed into a single fiber. It forms hydrogen bonds with a large number of hydroxyl groups on the surface of the cellulose fiber and is tightly and uniformly combined into a three-dimensional network. The paper is able to meet the requirements of high-performance papermaking with good formation.

Generally speaking, due to the existence of certain pores, the stress of the paper sheet is dispersed to a certain extent when it is loaded, so that it can bear a large load. However, the porosity is too large and the bonding between fibers is poor. When the paper sheet is under load, although the load can be effectively transmitted through the fibers and the bonding between fibers, when there are large pores, they will also be around the large pores. A stress-amplifying effect is produced, and the weaker fibers or fiber bonds are destabilized and broken. However, GA/EDA-PET perfectly makes up for the problem of large pores, but low load resistance (*i.e.* low strength). Due to its excellent strength and ability to combine with plant fibers, it can fully guarantee the strength requirements under the premise of large pore size and high porosity (60.30%). However, since the skeleton of paper strength is mostly provided by a large number of hydrogen bonds of plant fibers, the dosage of GA/EDA-PET as a reinforcing material should not be too high.

Effect of GA/EDA-PET addition on the performance of liner paper

Indexes of wet strength and air permeability are important for the performance of liner paper. Improvements to the performance of liner paper can be made by adding hydrophilic modified polyester staple fiber. The beating degree of the hardwood and softwood pulp used is 24 °SR and 32 °SR, respectively. The air permeability has different degrees of improvement with different proportions of hydrophilic polyester staple fiber replacing hardwood and softwood pulps (Figs. 5a and 5b). This is because the appearance of this polyester staple fiber is very smooth, with high air permeability and low air resistance, which is conducive to the passage of gas, liquid, and other media, which reduces pressure loss. In addition, the length of polyester staple fiber is longer than that of plants. The fiber is long, has more cross-holes, and larger porosity. The base paper is made from hardwood and softwood pulps with a ratio of 8:2. When 5% hardwood pulp is replaced by hydrophilic polyester staple fiber, the added amount is small and the hydrophilic polymer ester staple fiber has higher strength and slightly higher wet strength. The hydrophilic polyester staple fiber has a large number of hydroxyl groups on its rough and uneven surface. It is easy to form hydrogen bonds with plant fibers and its dispersion is less than that of the unmodified polyester staple fiber. The fiber is evenly bonded and the paper structure is tight. However, the wet strength cannot be increased by only increasing the hydrogen bonding as the improvement of wet strength depends on the formation of covalent bonds. The wet strength decreases only slightly as the hydrophilic polyester becomes shorter with the increase of fiber dosage.

Anti-mildew and antibacterial properties of laboratory-made lining paper

After standing at 60 °C and low relative humidity (15%RH~75%RH) for 48~168 h, the liner paper (Paper C) basically does not get moldy, and when the relative humidity reaches 90% RH, after 120 h, the liner paper reaches the C-level mildew situation: that is, when the concentrated beam is not more than 152 mm away from the sample, more foggy mildew is observed with the naked eye. Experiments have shown that, in moist environments, the liner paper can meet the required mildew resistance requirements.

The “sandwich” interlayer contact test method was used to characterize the antibacterial effect of the paper. Figure 5c shows the original paper (Paper A) and mixed GA/EDA after different contact times. The antibacterial effect of PET fiber paper (Paper B) and the backing paper (Paper C) with added antibacterial agent. The three kinds of paper have different antibacterial effects on *Staphylococcus aureus* and *E. coli* O157:H7. The antibacterial rate against *Staphylococcus aureus* and *E. coli* only reached 56.49% and 58.39% after the original paper contacted the bacteria for 30 minutes, while the same parameter reached 71.02% and 75.87% for the paper with 20% GA/EDA-PET fiber. This is because the gallic acid has antibacterial effects and the phenolic hydroxyl group helps

polyphenols to function through the cell membrane and interfere with the structure and function of the bacterial cell membrane.[19] The liner paper made with the addition of an antibacterial agent has an antibacterial rate of 100% and 95.84% against *Staphylococcus aureus* and *E. coli*.

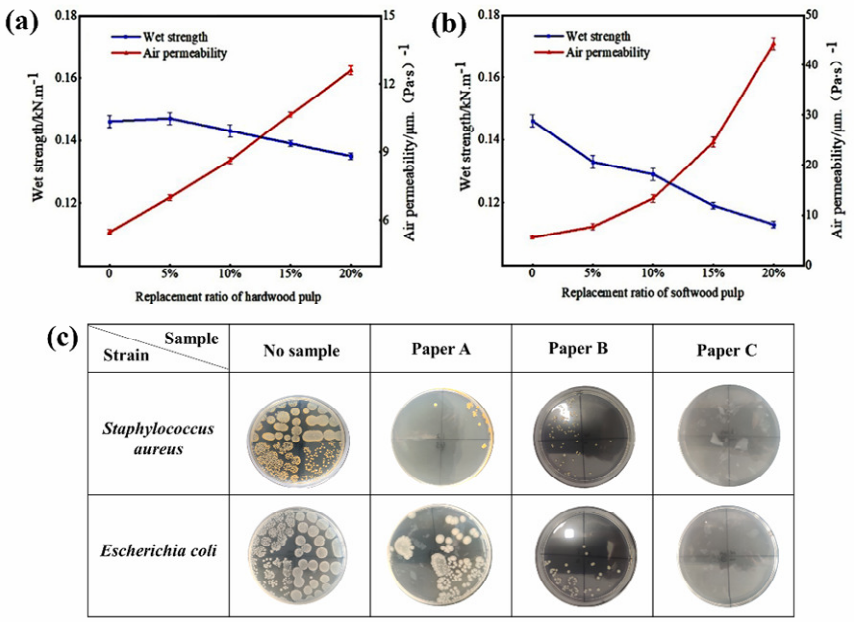

Figure 5: Influence of GA/EDA-PET fiber addition on paper properties (a), (b); Antibacterial performance of different papers towards two strains (c)

Table 3
Comparison of physical properties of liner paper

Property	Taiwan, China	Japan	Paper A	Paper C
Weight, $g.m^{-2}$	60.0	60.0	60.0	60.0
Thickness, mm	0.101	0.062	0.078	0.083
Tightness, $g.cm^{-3}$	0.60	0.96	0.77	0.72
Wet strength, $kN.m^{-1}$	0.640	0.830	0.146	0.720
Air permeability, $\mu m.(Pa{\cdot}s)^{-1}$	24.30	2.58	5.47	30.99
Tensile strength, $kN.m^{-1}$	—	—	3.429	2.871
Bursting index, $kPa.m^2.g^{-1}$	2.560	5.560	3.206	2.986
Paper conductivity, μs/cm	—	—	53.0	27.0

Physical properties of laboratory-made lining paper

Chinese Taiwan's liner paper has a low wet strength, high air permeability and cannot be stored for long periods of time in humid environments (Table 3). Japanese liner paper has a high wet strength, but low air permeability and is prone to water production. Gas promotes the growth of mold on the glass. The air permeability of the liner paper made in our laboratory is better than those of the Taiwanese and Japanese liner papers. The wet strength is slightly lower than that of the Japanese liner paper, but better than that of the Taiwanese liner paper, while the mixed hydrophilic modified polyester fiber has antibacterial properties and mildew resistance.

CONCLUSION

The surface of PET fiber undergoes the reaction of gallic acid and ethylenediamine to form a co-deposited coating under an alkaline Tris buffer. The surface changes from a smooth structure to a large fluffy, curved and uneven

layered aggregate structure. The introduction of polar groups and the increase of the surface roughness of the fiber improved its hydrophilicity and water dispersibility, which allowed its application for the preparation of liner paper. The optimal conditions for the co-deposition reaction were found to be a GA mass concentration of 0.8 g/L, a GA/EDA mass ratio 4:1, and a reaction time of 6 h. The wet strength of the laboratory-made liner paper is 0.72 kN/m, the air permeability is 30.99 μm.(Pa·s)$^{-1}$, while its antibacterial rate against *Staphylococcus aureus* and *E. coli* reached 100% and 95.84%. It maintains good mildew resistance in moist environments. These results show that this simple and environmentally friendly modification method can effectively improve the wettability of PET fibers and that GA/EDA-PET significantly improves the performance of liner paper, providing new ideas for the preparation of liner materials.

ACKNOWLEDGEMENT: This research work was financially supported by the State Key Laboratory of Biobased Materials and Green Papermaking, Qilu University of Technology, Shandong Academy of Sciences under Foundation Grant (KF201905); Guangxi Key Laboratory of Clean Pulp & Papermaking and Pollution Control, College of Light Industry and Food Engineering, Guangxi University under Foundation Grant [No. 2019KF03]; Guizhou Science & Technology Supporting Plan under Foundation Grant ([2019]2860); Support Plan for Science & Technology Top Talents in High Schools of Guizhou Province under Foundation Grant ([2018]079).

REFERENCES

[1] J. M. Delgado, D. Nunes, E. Fortunato, C. A. T. Laia, L.C. Branco *et al*., *Corros. Sci*., **118**, 109 (2017), https://doi.org/10.1016/j.corsci.2017.01.027

[2] A. Sivakumar, R. Murugan and S. Periyasamy, *Mater. Technol*., **31**, 286 (2016), https://doi.org/10.1179/1753555715Y.0000000055

[3] Z. Ge, H. Yue and R. Sun, *Constr. Build. Mater*., **93**, 851 (2015), http://dx.doi.org/10.1016/j.conbuildmat.2015.05.081

[4] J. Wu, G. Cai, J. Liu, H. Ge and J. Wang, *Appl. Surf. Sci*., **295**, 150 (2014), http://dx.doi.org/10.1016/j.apsusc.2014.01.019

[5] F. Abdelghaffar, R. A. Abdelghaffar, U. M. Rashed and H. M. Ahmed, *Environ. Sci. Pollut. R*., **27**, 28949 (2020), https://doi.org/10.1007/s11356-020-09081-9

[6] P. K. M. Adnan and L. Sreejith, *Mater. Lett*., **313**, 131705 (2022), https://doi.org/10.1016/j.matlet.2022.131705

[7] M. Saran, A. Kumar, M. Mathur and A. Bagaria, *Mater. Lett*., **304**, 130662 (2021), https://doi.org/10.1016/j.matlet.2021.130662

[8] M. Zhang, L. Jin, Y. Zhai, C. Cheng, F. Yan *et al*., *Compos. Commun*., **26**, 1007990 (2021), https://doi.org/10.1016/j.coco.2021.100790

[9] H. Zhang, D. Zhou, F. Yang, Z. Qian, C. Li *et al*., *J. Chromatogr. B*., **1124**, 7 (2019), https://doi.org/10.1016/j.jchromb.2019.05.031

[10] H. V. Walters and P. B. Adams, *J. Non. Cryst. Solids*, **19**, 183 (1975), https://doi.org/10.1016/B978-0-7204-0419-7.50022-6

[11] R. Sa, Y. Yan, Z. Wei, L. Zhang, W. Wang *et al*., *ACS Appl. Mater. Interfaces*, **6**, 21730 (2014), https://doi.org/10.1021/am507087p

[12] J. Gao, Z. Jin and Z. Pan, *Polym. Degrad. Stab*., **97**, 1838 (2012), https://doi.org/10.1016/j.polymdegradstab.2012.05.015

[13] D. R. Dreyer, D. J. Miller, B. D. Freeman, D. R. Paul and C. W. Bielawski, *Langmuir*, **28**, 6428 (2012), https://doi.org/10.1021/la204831b

[14] X. Li, Z. Yu, Q. Chen, S. Yang, F. Li *et al*., *Mater. Technol*., **34**, 213 (2019), https://doi.org/10.1080/10667857.2018.1548116

[15] Q. Lu, D. X. Oh, Y. Lee, Y. Jho, D. S. Hwang *et al*., *Angew. Chem. Int. Ed*., **52**, 3944 (2013), https://doi.org/10.1002/anie.201210365

[16] M. A. Gebbie, W. Wei, A. M. Schrader, T. R. Cristiani, H. A. Dobbs *et al*., *Nat. Chem*., **9**, 723 (2017), https://doi.org/10.1038/nchem.2720

[17] K. V. Pillai and S. Renneckar, *Biomacromolecules*, **10**, 798 (2009), https://doi.org/10.1021/bm801284y

[18] D. A. Dougherty, *Acc. Chem. Res*., **46**, 885 (2013), https://doi.org/10.1021/ar300265y

[19] L. J. Nohynek, H. Alakomi, M. P. Kähkönen, M. Heinonen, I. M. Helander *et al*., *Nutr. Cancer*, **54**, 18 (2006), https://doi.org/10.1207/s15327914nc5401_4